タイトル Title	Enhanced Performance of Sn4P3 Electrode Cycled in Ionic Liquid Electrolyte at Intermediate Temperature as Na‐Ion Battery Anode
著者 Auther(s)	Usui, Hiroyuki; Domi, Yasuhiro; Nishida, Haruka; Yamaguchi, Kazuki; Yamagami, Ryota; Sakaguchi, Hiroki
掲載誌・巻号・ページ Citation	ChemistrySelect , 3 (29) : 8462 - 8467
刊行日 Issue Date	2018-08-01
資源タイプ Resource Type	学術雑誌論文 / Journal Article
版区分 Resource Version	著者版 / Author
権利 Rights	© 2018 Wiley‐VCH Verlag GmbH & Co. KGaA, Weinheim
DOI	10.1002/slct.201801517
URL	http://repository.lib.tottori-u.ac.jp/6419

ARTICLE

Enhanced performance of Sn_4P_3 electrode cycled in ionic liquid electrolyte at intermediate temperature as Na-ion battery anode

Hiroyuki Usui,[a],[c] Yasuhiro Domi,[a],[c] Haruka Nishida,[a],[c] Kazuki Yamaguchi,[a],[c] Ryota Yamagami,[b],[c] and Hiroki Sakaguchi,*[a],[c]

Abstract: Charge–discharge performances of Sn_4P_3 anodes for Na-ion battery were evaluated in an ionic liquid electrolyte using *N*-methyl-*N*-propylpyrrolidinium bis(fluorosulfonyl)amide at intermediate temperatures of 60 and 90 °C. At these temperatures, the anode showed extra capacities based on the full sodiation of Sn in a potential range below 0.2 V vs. Na^+/Na because its slow kinetics was improved by elevating operation temperature. Under the current density of 0.1 A g^{-1} (0.08 *C*), the Sn_4P_3 anode at 60 °C exhibited a large capacity of 750 mA h g^{-1} at the 120th cycle and high Coulombic efficiencies above 99% after the 5th cycle. On the other hand, the efficiency degraded at 90 °C by the electrolyte decomposition. At 60 °C, the anode attained an excellent rate performance with capacity of 250 mA h g^{-1} even at 3 A g^{-1} (2.65 *C*). These results demonstrated the promising operation at intermediate temperature at around 60 °C for Sn_4P_3 anode in ionic liquid electrolyte.

Introduction

Demands for stationary energy storage systems have been recently growing by applications for renewable energy and smart grid. Na-ion batteries (NIBs) have emerged as one of the potential alternatives for Li-ion batteries (LIBs) because of the huge abundant sodium resource and its low cost.[1,2] From the viewpoint of operation mechanism as rechargeable batteries, NIB is very similar to LIB. Charge–discharge reactions occur by insertion–extraction of alkali-metal ions into/from electrode active materials of these batteries. The LIB electrode materials can provide beneficial references for developing the NIB electrode materials because many Na-ion insertion hosts have their roots in Li-ion insertion hosts. The larger size and different bonding characteristics of Na ions, however, influence the thermodynamic and/or kinetic properties of NIB, which leads to unexpected behavior in electrochemical performance and reaction mechanism, compared to LIB.[3] For instance, graphite in practical use for LIB anode does not show reversible charge–discharge reactions as NIB anode.[4] Thus, NIB active materials require an appropriate material design, which is similar to that of LIB but different.

Hard carbons have disordered layered structure with nanopores, which has been reported to be suitable for reversible insertion and extraction of Na ions.[5-7] Komaba *et al.* have reported that the hard carbon electrode exhibited a good cycle stability and reversible capacities of 220–260 mA h g^{-1} for 100 charge–discharge cycles. In the most recently, the hard carbon electrode has maintained the reversible capacity of as high as 320 mA h g^{-1} for 100 cycles.[8] Although hard carbon is one of the promising candidates as NIB anode material, there are considerable interests in other anode materials showing better cyclability and higher capacity.

As NIB anode materials, many researchers have particularly focused on titanium oxides, phosphorus (P), and tin (Sn). Titanium oxides can work as host materials for Na ions at lower electrode potentials than those of other transition metal oxides. Tarascon and Palacín have reported reversible Na-insertion/extraction of $Na_2Ti_3O_7$ at a low potential of 0.3 V vs. Na^+/Na.[9] Rudola *et al.* have explored Na-ion storage in the structurally similar $Na_2Ti_6O_{13}$, demonstrating a reversible uptake by a solid solution mechanism at an average potential of 0.8 V vs. Na^+/Na.[10] Although these sodium titanates are very promising as host materials, those have still suffered from their poor electronic conductivities as electrode materials.

P, Sn,[11] Sb,[12] and Bi[13] are very attractive elements showing alloying–dealloying reactions because those have high theoretical capacities (Na_3P: 2596 mA h g^{-1}, $Na_{15}Sn_4$: 847 mA h g^{-1}, Na_3Sb: 660 mA h g^{-1}, Na_3Bi: 385 mA h g^{-1}). In particular, the theoretical capacities of P and Sn are outstanding. On the other hand, P and Sn have serious disadvantages. The two elements show significant volume expansions of about 500% when fully sodiated. Owing to such severe volume expansion/contraction, P electrode and Sn electrode cause the void space formation in active material layer and the electrode disintegration. In addition, a poor electronic conductivity of Na_3P phase disturbs electrode reactions of P electrodes. Small Sn nanoparticles react and merge together to form large agglomerates, resulting in acceleration of the disintegration. Consequently, P electrode and Sn electrode generally show a rapid capacity fading and a short cycle life.

To solve these problems, Hagiwara, Nohira, and Yamamoto have conducted systematic studies for several binary alloys consisting of Sn and transition metals, Cu–Sn,[14] Ni–Sn,[15] and

[a] Dr. H. Usui, Dr. Y. Domi, H. Nishida, K. Yamaguchi, and Prof. H. Sakaguchi
Department of Chemistry and Biotechnology, Graduate School of Engineering, Tottori University
4-101 Minami, Koyama-cho, Tottori 680-8552, Japan
E-mail*: sakaguch@tottori-u.ac.jp
[b] R. Yamagami
Course of Chemistry and Biotechnology, Department of Engineering, Graduate School of Sustainability Science, Tottori University
4-101 Minami, Koyama-cho, Tottori 680-8552, Japan
[c] Dr. H. Usui, Dr. Y. Domi, H. Nishida, K. Yamaguchi, R. Yamagami, and Prof. H. Sakaguchi
Center for Research on Green Sustainable Chemistry, Tottori University
4-101 Minami, Koyama-cho, Tottori 680-8552, Japan

Supporting information for this article is given via a link at the end of the document.

Fe–Sn.[16] The results of their studies indicate that Na-inactive elements (Cu, Ni, and Fe) are effective for improving the rapid capacity fading of Sn. Vogta and Villevieille have reported that $MnSn_2$ exhibited a stable cyclability based on its conversion reaction in addition to the sodiation–desodiation reactions of Sn.[17] As phosphorus-based materials, Zhao *et al.* have demonstrated that CuP_2 is capable of reversible sodiation–desodiation based on the conversion mechanism.[18] On the other hand, the authors have applied two kinds of unique material designs, (i) the doping of impurity element and (ii) the formation of various compounds. As the result, we have succeeded to newly develop many anode materials: Nb-doped rutile TiO_2,[19-21] SiO,[22] SnO,[23] $LaSn_3$,[24] Sn_4P_3,[25,26] InP,[27] GeP,[27] and SiP.[27] A series of the material development has revealed that the best anode performance was obtained for Sn_4P_3, a compound of two elements with high Na-activity. In 2014, Yang[28] and Kim[29] also have revealed that Sn_4P_3 electrodes exhibited good cycling performances in conventional organic electrolytes. In 2017, Wang *et al.* have reported an improved performance by their unique material design: a composite of Sn_4P_3 and Na-inactive TiC.[30] They obtained capacities of 300 mA h g^{-1} for 100 cycles under the charge–discharge current density of 100 mA g^{-1}.[30] Ahead of their reports, the authors have developed Sn_4P_3 as a potential anode material in 2013.[31] In addition, the authors have firstly discovered that it exhibited an outstanding cycling performance by choosing an optimal ionic liquid electrolyte comprised of *N*-methyl-*N*-propylpyrrolidinium (Py13 or C_3C_1pyrr) cation and bis(fluorosulfonyl)amide (FSA) anion.[26] The Sn_4P_3 electrode achieved a high capacity of 750 mA h g^{-1} even at the 200th cycle under 50 mA g^{-1} at room temperature.

As one of the reasons for the excellent property of this anode material, we suggest a complementary effect of Sn and P.[25,26] After its phase separation at the first sodiation, an Sn phase functions as a conducting pathway to activate reversible desodiation of a nonconductive Na_3P, whereas the Na_3P phase provides a shield matrix preventing Sn aggregation.[25,28,29] We have confirmed that the first desodiation of Sn_4P_3 forms nanostructured domains in which crystalline Sn nanoparticles are dispersed in the amorphous-like P matrix.[26]

The other reason is related to the properties of the ionic liquid electrolyte. As an important role of the ionic liquid electrolyte, the authors have proposed the construction of a stable interface between electrode and electrolyte.[24,26] Py13 (C_3C_1pyrr) cations have a high electrochemical stability.[32] In charge reaction, FSA anions decompose to form a chemically stable surface layer consisting of NaF and $NaSO_2F$.[33] The cations and the surface layer can suppress a continuous decomposition of electrolyte, and can improve charge–discharge efficiency. In addition, FSA-based ionic liquids have relatively low viscosity and high ionic conductivity among various ionic liquids because of flexible coordination structure of FSA anions.[34] Nevertheless, the conductivity of this ionic liquid at room temperature is still inferior to that of conventional organic electrolyte.[35] The elevation of the operating temperature is expected to improve the ion transport in the electrolyte.[36] By contrast, the surface layer becomes more unstable with increasing the temperature because it may dissolve into the electrolyte more easily, which possibly degrades the anode performance of Sn_4P_3 electrode. It is very important to actually evaluate the performance at elevated temperatures. Intermediate temperatures between 60 °C and 90 °C can be easily realized by using waste heat from factories and households because the waste heat is obtained with a very low cost. Therefore, in this study, we evaluated the performance of the Sn_4P_3 anodes in the ionic liquid electrolyte at the intermediate temperatures.

Results and Discussion

A mechanical ball milling treatment was conducted for Sn and P powders to form Sn_4P_3 powder. An X-ray diffraction analysis confirmed that a desired active material of Sn_4P_3 was obtained (Fig. S1).

Galvanostatic charge–discharge curves in the initial five cycles were shown in Fig. S2–S5 for Sn_4P_3 electrodes at the temperatures of 0, 30, 60, and 90 °C. Irreversible capacities were observed at the first charge–discharge cycles. As the authors have reported,[26] Sn_4P_3 electrodes show the irreversible reaction at the first cycles by its phase separation. Coulombic efficiencies at the first cycles were 55.9%, 80.0%, 84.6%, and 82.5% at the temperatures of 0, 30, 60, and 90 °C, respectively (Fig. S2–S5). The efficiencies steeply rose as high as 98% by the 5th cycles. This indicates that sufficiently reversible electrode reactions took place at the 5th cycles. Figure 1 shows the charge (sodiation) and discharge (desodiation) potential profiles at the 5th cycles evaluated in the ionic liquid electrolyte at various temperatures. At 0 °C, a low charge capacity of 220 mA h g^{-1} was obtained. It is suggested that the electrode reaction of Sn_4P_3 was kinetically restricted by the poor electrolyte conductivity of 1.5 mS cm^{-1} at 0 °C. The charge capacity was significantly increased in the temperature range from 0 to 60 °C, whereas no remarkable increase was observed at 90 °C. The charge curve profile between 2.0 and 0.2 V vs. Na^+/Na at 30 °C almost entirely coincided with those at 60 and 90 °C. In the potentials below 0.2 V vs. Na^+/Na, charge capacities more than 400 mA h g^{-1} were produced at 60 and 90 °C, which was never confirmed at 30 °C.

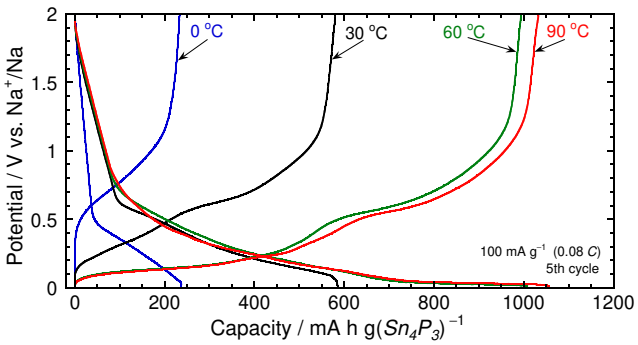

Figure 1. Charge–discharge curves of Sn_4P_3 electrode in the 5th cycles evaluated by using ionic liquid electrolyte (NaFSA/Py13-FSA) at various temperatures under the current density of 100 mA g^{-1}.

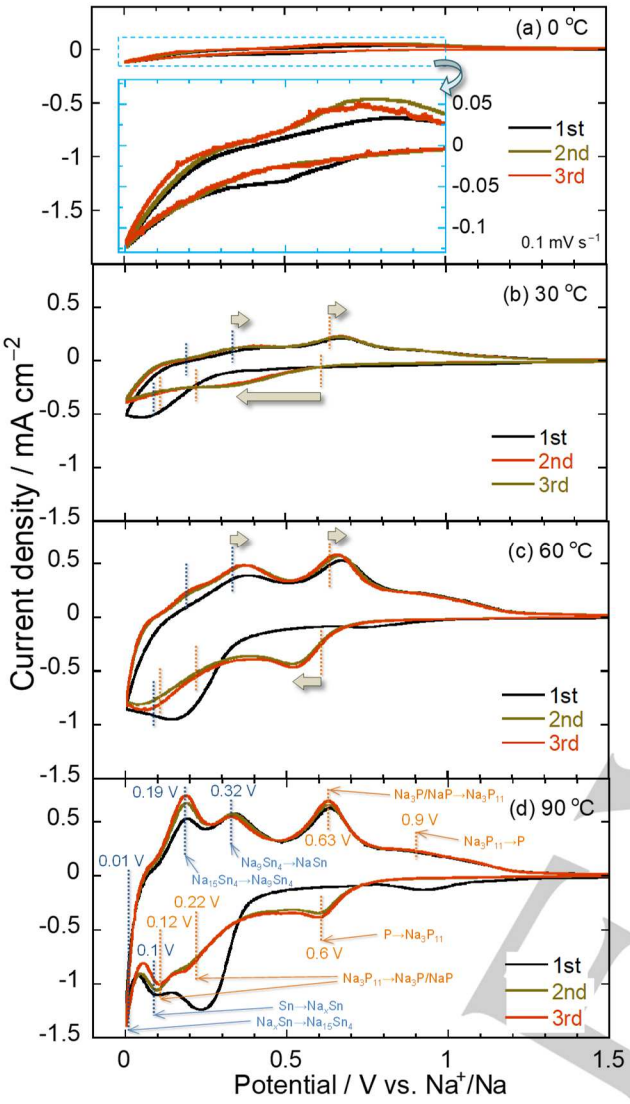

Figure 2. Cyclic voltammograms of Sn_4P_3 electrodes at different temperatures.

Figure 2 represents cyclic voltammograms of Sn_4P_3 electrodes in the ionic liquid electrolytes of NaFSA/Py13-FSA at various temperatures. At 0 °C, the current densities of cathodic and anodic peaks were very small. It is suggested that the low conductivity of electrolyte hindered the electrode reaction of Sn_4P_3. At the temperatures equal to or higher than 30 °C, CV profiles showed multiple peaks. The authors[26] and other groups[28,29] have revealed that a disproponation of Sn_4P_3 occurs at the first cycle to form elemental Sn and P, and that Sn and P individually react with Na ions in the subsequent cycles. As Sn's electrode reactions, Obrovac *et al.* have found four potential peaks originating from phase transformation between Sn, $NaSn_3$, NaSn, Na_9Sn_4, and $Na_{15}Sn_4$: the charge (sodiation) peaks appeared at around 0.43, 0.20, 0.08, and 0.05 V vs. Na^+/Na, while the discharge (desodiation) peaks were observed at around 0.14, 0.23, 0.55, and 0.65 V vs. Na^+/Na.[37,38] The three peaks at the higher potentials often merged into one peak owing to the slow kinetics of Na diffusion in Sn.[38,39] As the result, two kinds of sodiation reactions are observed:

$$Sn + xNa^+ + xe^- \rightarrow Na_xSn \quad (1),$$

$$Na_xSn + yNa^+ + ye^- \rightarrow Na_{15}Sn_4 \quad (2).$$

The authors also have previously confirmed two sodiation peaks at the potentials below 0.2 V vs. Na^+/Na.[24] As P's electrode reactions, Dahbi *et al.*[40] and Shimizu *et al.*[41] have reported that broad two or three peaks were observed for charge and discharge curves at 0.3–0.5 V and 0.5–0.8 V versus Na^+/Na, indicating the phase transformations between P, Na_3P_{11}, NaP, and Na_3P.[41,42] In this study, peak positions of the profile at 90 °C (Fig. 2(d)) well agreed with those of Sn electrodes[37-39] and P electrodes[40-42] previously reported. In the sodiation profile, cathodic peaks at 0.6, 0.22, and 0.12 V are attributed to phase transformation reactions of P→Na_3P_{11}, Na_3P_{11}→NaP, and NaP→Na_3P. Anodic peaks by their reverse reactions appeared at 0.9 and 0.63 V. Although there is an overlapping of peak profiles, we can recognize two cathodic peaks at 0.1 V (Sn→Na_xSn) and 0.01 V (Na_xSn→$Na_{15}Sn_4$). The reverse reactions were observed as anodic peaks at 0.32 and 0.19 V. There is an obvious difference in cathodic profiles between the first cycle and the following cycles. A broad cathodic peak at 0.9 V and a large one at 0.25 V were observed only at the first cycle, which probably originate from the cathodic decomposition of the electrolyte and the phase separation reaction of Sn_4P_3, respectively. When the temperature was decreased to 60 °C, the cathodic peak (P→Na_3P_{11}) at the 2nd and 3rd cycles were shifted toward lower potential, whereas the anodic peaks were shifted to higher potential side. In addition, at 30 °C, the shift of cathodic peak became more pronounced. These results indicates that there was an overpotential for the sodiation of phosphorus by decrease in electronic conductivity of the electrode, which is probably caused by the lost of the Sn's complementary effect as an electronic conductive matrix. Note that the cathodic peak intensity at 0.01 V was reduced with decreasing the temperature from 90 to 30 °C. We consider that the $Na_{15}Sn_4$ formation reaction was considerably suppressed at the lower temperatures because of the polarization. The anodic peak intensity at 0.19 V ($Na_{15}Sn_4$→Na_9Sn_4) was also reduced with decreasing the temperature, supporting our consideration. A similar temperature-dependence has been reported for a high-capacity Si electrode as LIB anode.[43] Haruta *et al.* have observed a large polarization and a suppressed lithiation for charge–discharge reaction of Si at a low temperature of –5 °C, whereas the full lithiation reaction (Si→$Li_{15}Si_4$) at a low potential was confirmed for an elevated temperature of 60 °C.[43] They explained this reason as follows: the full lithiation and the decreased polarization were caused by improving the Si's slow kinetics and the high electrolyte-resistance at low temperature. From the high-capacity point of view, the electrode reaction (Na_xSn→$Na_{15}Sn_4$) at the low potential should be very important.

Figure 3 compares charge–discharge curves focusing on the lower potential ranges. By subtracting 410 and 450 mA h g^{-1} from the desodiation capacities at 60 and 90 °C, we can compare the desodiation curve profiles at lower potential ranges. Interestingly, the sodiation–desodiation profiles above 0.2 V vs. Na^+/Na at 60

and 90 °C almost completely coincided with that at 30 °C. This comparison demonstrated that the extra capacities of 410 and 450 mA h g^{-1} were produced at the low potential regions form 0 to 0.2 V vs. Na^+/Na, which is a benefit of the elevated temperature operation.

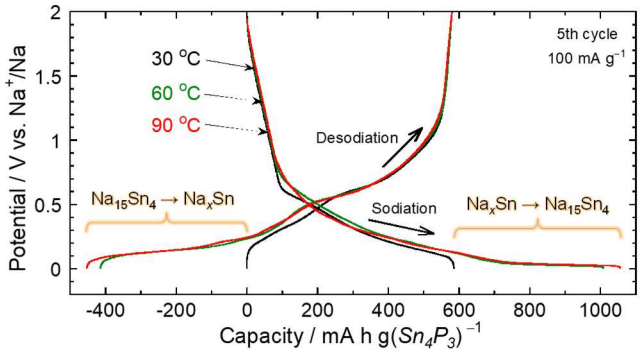

Figure 3. Charge–discharge curves of Sn_4P_3 electrode at the 5th cycles under the current densities of 100 mA g^{-1}. For desodiation curves at 60 and 90 °C, the capacities of 410 and 450 mA h g^{-1} were subtracted so that the curve profiles can be compared.

The extra capacities are attributed to the full sodiation of Sn ($Na_xSn \rightarrow Na_{15}Sn_4$) and its reverse reaction ($Na_{15}Sn_4 \rightarrow Na_xSn$). Even at the low temperature of 30 °C, the extra capacity could be obtained by reducing the charge–discharge current density from 100 to 50 mA g^{-1} (Fig. S6). This indicates that slow kinetics of Sn's sodiation reaction prohibited its full sodiation at 30 °C. It is considered that the elevation of operation temperature can improve the Sn's slow kinetics.

This consideration was supported by results of an electrochemical impedance spectroscopic analysis (Fig. S7). The charge-transfer resistance (R_{ct}) at the full sodiation state was as large as 157 Ω when the temperature was 0 °C, whereas it was drastically reduced to 8.0 Ω at 30 °C. Furthermore, the resistance showed lower values of 2.3 and 1.7 Ω at 60 and 90 °C, respectively.

Figure 4 shows cycling performances of Sn_4P_3 electrode cycled under the current density of 100 mA g^{-1} at various temperatures. In the range of 0 to 60 °C, the discharge capacity was remarkably increased with increasing temperature. Especially at 60 °C, the Sn_4P_3 electrode exhibited very large capacities of approximately 1000 mA h g^{-1} in the initial cycles. It is notable that the capacities are comparable to the Sn_4P_3's theoretical capacity of 1133 mA h g^{-1}. This is probably because the electrode reaction of Sn_4P_3 progressed more efficiently at the elevated temperature by the reduced reaction resistance as well as the enhanced electrolyte conductivity. At the 120th cycle, 750 mA h g^{-1} was attained. Although the conductivity showed a further enhancement at 90 °C, no significant improvement in the discharge capacity was observed. In addition to this, the capacities after the 75th cycle were inferior to those at 60 °C. As mentioned above, the initial Coulombic efficiencies at 30–90 °C were 80–85% (Fig. S2–S5). The relatively low efficiencies are attributed to the phase separation reaction of Sn_4P_3 in the charge process at the initial cycle[26]. At the second cycle, the efficiencies remarkably rose up to 97–98% because there was no phase separation. Coulombic efficiencies after the 5th cycle were more than 99% at 30 to 60 °C. By contrast, it remained only 98% at 90 °C. The decomposition of the electrolyte probably occurred owing to such high temperature.

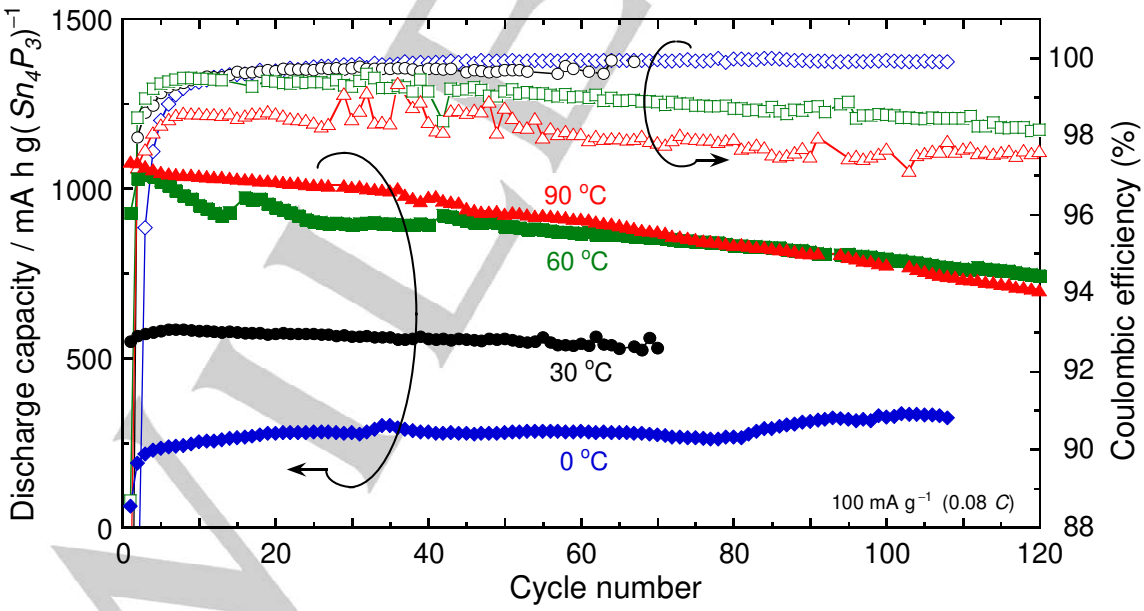

Figure 4. Variation in discharge capacity and Coulombic efficiency of Sn_4P_3 electrode cycled in NaFSA/Py13-FSA at various temperatures. The values in parentheses indicate the conductivity of the ionic liquid electrolytes at the temperatures.

Figure 5 gives results of rate capability measurements at various current densities. At a high current density of 1 A g^{-1} (0.88 *C*-rate), the electrode lost almost all its discharge capacity at 0 °C, whereas it maintained 250 mA h g^{-1} at 30 °C. In contrast, the electrode exhibited excellent rate capabilities with the large capacities of 500 mA h g^{-1} at 60 and 90 °C. At 3 A g^{-1} (2.65 *C*-rate), the capacity was 250 mA h g^{-1} at 60 °C, which is superior to that of 230 mA h g^{-1} at 90 °C. This capacity corresponds to that of a hard carbon electrode under a very low current density of 0.2 A g^{-1} at room temperature.[44] The excellent rate performance demonstrated that Sn_4P_3 anode in ionic liquid electrolyte at intermediate temperature around 60 °C is very promising for high-performance NIB.

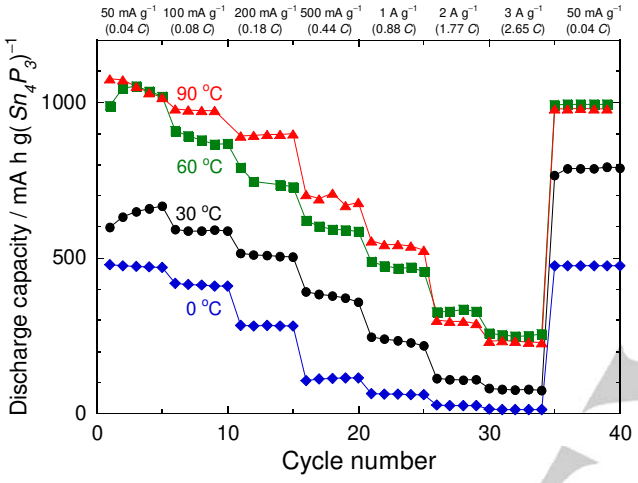

Figure 5. Rate performances of Sn_4P_3 electrode in NaFSA/Py13-FSA at various temperatures.

Conclusions

We investigated charge–discharge performances of Sn_4P_3 anodes in an ionic liquid electrolyte of NaFSA/Py13-FSA at intermediate temperatures of 60 and 90 °C. The electrode showed extra capacities based on the full sodiation of Sn in a potential range below 0.2 V vs. Na^+/Na at 60 and 90 °C because its slow kinetics could be improved by elevating operation temperature from 30 °C. Under the charge–discharge current density of 0.1 A g^{-1} (0.08 *C*), the Sn_4P_3 electrode at 60 °C exhibited a large capacity of 750 mA h g^{-1} at the 120th cycle and high Coulombic efficiencies above 99% after the 5th cycle. On the other hand, the degradation of efficiency was observed at 90 °C. The reason is probably the electrolyte decomposition owing to too high temperature. Even at 3 A g^{-1} (2.65 *C*), a large capacity of 250 mA h g^{-1} was attained at 60 °C. From the above results, it was confirmed that the Sn_4P_3 electrode exhibited remarkable NIB anode performances with large capacities, high Coulombic efficiencies, and better rate capabilities in the ionic liquid electrolyte at the intermediate temperature range of about 60 °C.

Experimental Section

An active material powder of Sn_4P_3 was synthesized by a mechanical alloying (MA) using commercially available tin powder (99.99%, Rare Metallic) and red phosphorous powder (99.8%, Wako Pure Chemical). The MA treatment was conducted by a Fritsch planetary-type high-energy ball mill (Fritsch Pulverisette P6) and a stainless steel vessel. The weight ratio of the active material and stainless steel balls was 1:30. The MA duration time and rotation speed were 10 hours and 380 rpm. The detailed procedure has been described in previous paper.[26] The active material obtained has a crystal structure of trigonal Sn_4P_3 (Inorganic Crystal Structure Database, ICSD No. 03-066-0017), which was confirmed by analysis using an X-ray diffraction (XRD, Ultima IV, Rigaku) as shown in Fig. S1. Electrodes were prepared by using of Sn_4P_3/acetylene black/carboxymethyl cellulose/styrene-butadiene rubber with the weight ratio of 70/15/10/5 wt.%. The current collector was Al foil. The loading amount and the film thickness of active material layer were 1.2 mg cm^{-2} and 10 µm, respectively. Electrochemical measurements of Na-insertion (charge) and Na-extraction (discharge) were carried out for 2032-type coin half cells consisted of Na metal sheets and glass fiber separators. We used ionic liquid electrolytes of 1.0 mol dm^{-3} NaFSA-dissolved in Py13-FSA. Galvanostatic charge–discharge tests were performed using an electrochemical measurement system (HJ-1001 SM8A, Hokuto Denko Co., Ltd.) under the current density of 100 mA g^{-1} (0.088 *C*) with potential ranges of 0.005–2.000 V vs. Na^+/Na. The measurements were conducted at a low temperature (0 °C), room temperature (30 °C), and intermediate temperatures (60 and 90 °C). A cyclic voltammetry (CV) and an electrochemical impedance spectroscopic (EIS) analysis were performed by using an impedance analyzer (CompactStat.h 20250e, Ivium Technologies). The EIS measurements were done at 0.005 V vs. Na^+/Na with the potential amplitude of 10 mV in the frequency range of 10 kHz–500 Hz. Nyquist plots were analyzed by using Randles equivalent circuit (Fig. S8) containing solution resistance (R_{sol}), surface film resistance (R_{sf}), and charge transfer resistance (R_{ct}). The conductivities of the electrolytes were evaluated for a symmetric cell of two platinum plates (Fig. S9), demonstrating that the conductivities at 0, 30, 60, and 90 °C were 1.5, 5.7, 12.7, and 20.0 mS cm^{-1}, respectively. As we expected, the conductivity was improved with increasing the temperature. The results basically agree with the values reported by Ding *et al.*[36]

Acknowledgements

This study was partially supported by Advanced Low Carbon Technology Research and Development Program (ALCA, 16200610802), Joint Usage/Research Program on Zero-Emission Energy Research, Institute of Advanced Energy, Kyoto University (ZE29A-14, ZE30A-05, ZE30A-06), and Japan Society for the Promotion of Science (JSPS) KAKENHI (Grant Number 17H03128, 17K17888, 16K05954).

Keywords: Na-ion battery • Anode materials • Tin phosphide (Sn_4P_3) • Ionic liquid electrolyte • Intermediate temperature

[1] N. Yabuuchi, K. Kubota, M. Dahbi, S. Komaba, *Chem. Rev.* **2014**, *114*, 11636–11682.

[2] D. Kundu, E. Talaie, V. Duffort, L. F. Nazar, *Angew. Chem. Int. Ed.* **2015**, *54*, 3431–3448.

[3] S. Y. Hong, Y. Kim, Y. Park, A. Choi, N.-S. Choi, K. T. Lee, *Energy Environ. Sci.* **2013**, *6*, 2067–2081.

[4] P. Ge and M. Fouletier, *Solid State Ionics*, **1988**, *28–30*, 1172–1175.

[5] R. Alcántara, P. Lavela, G. F. Ortiz, J. L. Tirado, R. Menéndez, R. Santamaría, J. M. Jiménez-Mateos, *Carbon* **2003**, *41*, 3003–3013.
[6] S. Komaba, W. Murata, T. Ishikawa, N. Yabuuchi, T. Ozeki, T. Nakayama, A. Ogata, K. Gotoh, K. Fujiwara, *Adv. Funct. Mater.* **2011**, *21*, 3859–3867.
[7] M. Dahbi, T. Nakano, N. Yabuuchi, T. Ishikawa, K. Kubota, M. Fukunishi, S. Shibahara, J.-Y. Son, Y.-T. Cui, H. Oji, S. Komaba, *Electrochem. Commun.* **2014**, *44*, 66–69.
[8] M. Dahbi, M. Kiso, K. Kubota, T. Horiba, T. Chafik, K. Hida, T. Matsuyama, S. Komaba, *J. Mater. Chem.* **2017**, *5*, 9917–9928.
[9] P. Senguttuvan, G. Rousse, V. Seznec, J.-M. Tarascon, M. R. Palacín, *Chem. Mater.* **2011**, *23*, 4109–4111.
[10] A. Rudola, K. Saravanan, S. Devaraj, H. Gong, P. Balaya, *Chem. Commun.* **2013**, *49*, 7451–7453.
[11] L. Wu, H. Lu, L. Xiao, J. Qian, X. Ai, H. Yang, Y. Cao, *J. Mater. Chem. A* **2014**, *2*, 16424–16428.
[12] Y. Zhao and A. Manthiram, *Chem. Mater.* **2015**, *27*, 6139–6145.
[13] Y. Zhang, L. Fan, P. Wang, Y. Yin, X. Y. Zhang, N. Zhang, K. Sun, *Nanoscale* **2017**, *9*, 17694–17698.
[14] T. Yamamoto, T. Nohira, R. Hagiwara, A. Fukunaga, S. Sakai, K. Nitta, S. Inazawa, *Electrochim. Acta* **2014**, *135*, 60–67.
[15] T. Yamamoto, T. Nohira, R. Hagiwara, A. Fukunaga, S. Sakai, K. Nitta, *Electrochim. Acta* **2016**, *193*, 275–283.
[16] T. Yamamoto, T. Nohira, R. Hagiwara, A. Fukunaga, S. Sakai, K. Nitta, *Electrochim. Acta* **2016**, *211*, 234–244.
[17] L. O. Vogta and C. Villevieille, *J. Mater. Chem. A* **2016**, *4*, 19116–19122.
[18] F. Zhao, N. Han, J. Huang, J. Li, H. Ye, F. Chen, Y. Li, *J. Mater. Chem. A*, **2015**, *3*, 21754–21759.
[19] H. Usui, S. Yoshioka, K. Wasada, M. Shimizu, H. Sakaguchi, *ACS Appl. Mater. Interfaces* **2015**, *7*, 6567–6573.
[20] H. Usui, Y. Domi, S. Yoshioka, K. Kojima, H. Sakaguchi, *ACS Sustainable Chem. Eng.* **2016**, *4*, 6695–6702.
[21] H. Usui, Y. Domi, M. Shimizu, A. Imoto, K. Yamaguchi, H. Sakaguchi, *J. Power Sources* **2016**, *329*, 428–431.
[22] M. Shimizu, H. Usui, K. Fujiwara, K. Yamane, H. Sakaguchi, *J. Alloys Compd.* **2015**, *640*, 440–443.
[23] M. Shimizu, H. Usui, H. Sakaguchi, *J. Power Sources* **2014**, *248*, 378–382.
[24] H. Usui, Y. Domi, S. Ohshima, H. Sakaguchi, *Electrochim. Acta* **2017**, *246*, 280–284.
[25] H. Usui, T. Sakata, M. Shimizu, H. Sakaguchi, *Electrochemistry* **2015**, *83*, 810–812.
[26] H. Usui, Y. Domi, K. Fujiwara, M. Shimizu, T. Yamamoto, T. Nohira, R. Hagiwara, H. Sakaguchi, *ACS Energy Lett.* **2017**, *2*, 1139–1143.
[27] H. Usui, Y. Domi, R. Yamagami, K. Fujiwara, H. Nishida, H. Sakaguchi, *ACS Appl. Energy Mater.* **2018**, *1*, 306–311.
[28] J. Qian, Y. Xiong, Y. Cao, X. Ai, H. Yang, H, *Nano Lett.* **2014**, *14*, 1865–1869.
[29] Y. Kim, Y. Kim, A. Choi, S. Woo, D. Mok, N.-S. Choi, Y. S. Jung, J. H. Ryu, S. M. Oh, K. T. Lee, *Adv. Mater.* **2014**, *26*, 4139–4144.
[30] W. Wang, J. Zhang, D. Y. W. Yu, Q. Li, *J. Power Sources* **2017**, *364*, 420–425.
[31] H. Sakaguchi, T. Itoh, H. Usui, H. Furutani, *Jpn. Pattent Application*, JP2013133933. (Japanese Patent No. 6358871)
[32] H. Matsumoto, H. Sakaebe, K. Tatsumi, M. Kikuta, E. Ishiko, M. Kono, *J. Power Sources* **2006**, *160*, 1308–1313.
[33] M. Dahbi, M. Fukunishi, T. Horiba, N. Yabuuchi, S. Yasuno, S.; Komaba, *J. Power Sources* **2017**, *363*, 404–412.
[34] K. Fujii, H. Hamano, H. Doi, X. Song, S. Tsuzuki, K. Hayamizu, S. Seki, Y. Kameda, K. Dokko, M. Watanabe, Y. Umebayashi, *J. Phys. Chem. C* **2013**, *117*, 19314–19324.
[35] A. Ponrouch, D. Monti, A. Boschin, B. Steen, P. Johansson, M. R. Palacín, *J. Mater. Chem. A* **2015**, *3*, 22–42.
[36] C. Ding, T. Nohira, A. Fukunaga, R. Hagiwara, *Electrochemistry* **2015**, *83*, 91–94.
[37] L. D. Ellis, T. D. Hatchard, M. N. Obrovac, *J. Elecreochem. Soc.* **2012**, *159*, A1801–A1805.
[38] Z. Du, R. A. Dunlap, M. N. Obrovac, *J. Alloys Compd.* **2014**, *617*, 271–276.
[39] M. K. Datta, R. Epur, P. Saha, K. Kadakia, S. K. Park, P. N. Kumta, *J. Power Sources* **2013**, *225*, 316–322.
[40] M. Dahbi, N. Yabuuchi, M. Fukunishi, K. Kubota, K. Chihara, K. Tokiwa, X. F. Yu, H. Ushiyama, K. Yamashita, J.-Y. Son, Y.-T. Cui, H. Oji, S. Komaba, *Chem. Mater.* **2016**, *28*, 1625–1635.
[41] M. Shimizu, Y. Tsushima, S. Arai, *ACS Omega* **2017**, *2*, 4306–4315.
[42] M. Mortazavi, Q. Ye, N. Birbilis, N. V. Medhekar, *J. Power Sources* **2015**, *285*, 29–36.
[43] M. Haruta, T. Okubo, Y. Masuo, S. Yoshida, A. Tomita, T. Takenaka, T. Doi, M. Inaba, *Electorochim. Acta*, **2017**, *224*, 186–193.
[44] G. Hasegawa, K. Kanamori, N. Kannari, J. Ozaki, K. Nakanishi, T. Abe, *ChemElectroChem* **2015**, *2*, 1917–1920.

Entry for the Table of Contents

ARTICLE

Sn_4P_3 anodes were cycled in an ionic liquid electrolyte at intermediate temperatures for Na-ion battery. At 60 °C, the anode exhibited extra capacities and further enhanced performance. One of the reasons is the improved kinetics in the full sodiation reaction of Sn.

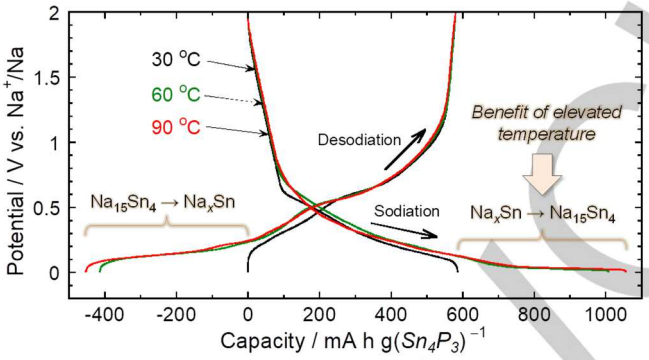

*Hiroyuki Usui, Yasuhiro Domi, Haruka Nishida, Kazuki Yamaguchi, Ryota Yamagami, and Hiroki Sakaguchi**

Page 1. – Page 6.

Enhanced performance of Sn_4P_3 electrode cycled in ionic liquid electrolyte at intermediate temperature as Na-ion battery anode